TU Delft

Delft University of Technology

Document Version
Final published version

Licence
Dutch Copyright Act (Article 25fa)

Citation (APA)
Babu, G., De Koninck, L., Rayner, S. G., de Jong, N., Glenny, R. W., & Averkiou, M. A. (2026). A Clinical Perspective and Review on the Use of the Subharmonic Signal of Ultrasound Contrast Agents for Noninvasive Pressure Estimation. *Ultrasound in Medicine and Biology*, *52*(8), 1446-1457. https://doi.org/10.1016/j.ultrasmedbio.2026.03.027

Important note
To cite this publication, please use the final published version (if applicable).
Please check the document version above.

Copyright
In case the licence states “Dutch Copyright Act (Article 25fa)”, this publication was made available Green Open Access via the TU Delft Institutional Repository pursuant to Dutch Copyright Act (Article 25fa, the Taverne amendment). This provision does not affect copyright ownership.
Unless copyright is transferred by contract or statute, it remains with the copyright holder.

Sharing and reuse
Other than for strictly personal use, it is not permitted to download, forward or distribute the text or part of it, without the consent of the author(s) and/or copyright holder(s), unless the work is under an open content license such as Creative Commons.

Takedown policy
Please contact us and provide details if you believe this document breaches copyrights.
We will remove access to the work immediately and investigate your claim.

This work is downloaded from Delft University of Technology.

Ultrasound in Medicine & Biology 52 (2026) 1446–1457

Contents lists available at ScienceDirect

Ultrasound in Medicine & Biology

journal homepage: www.elsevier.com/locate/ultrasmedbio

Review

A Clinical Perspective and Review on the Use of the Subharmonic Signal of Ultrasound Contrast Agents for Noninvasive Pressure Estimation

Gautam Babu [a,b], Lance De Koninck [b], Samuel G. Rayner [a], Nico de Jong [c,d], Robb W. Glenny [a], Michalakis A. Averkiou [b,*]

[a] Division of Pulmonary, Critical Care and Sleep Medicine, University of Washington, Seattle, WA, USA
[b] Department of Bioengineering, University of Washington, Seattle, WA, USA
[c] Biomedical Engineering, Erasmus Medical Center, Rotterdam, The Netherlands
[d] Department of Imaging Physics, Delft University of Technology, Delft, The Netherlands

ARTICLE INFO

Keywords:
Ultrasound contrast agents, Subharmonic imaging
Physiologic pressure estimation, Ambient pressure sensitivity, Subharmonic-aided pressure estimation, SHAPE

ABSTRACT

Changes in physiological pressures play a key role in the development and progression of human disease processes. Thus, the assessment of pressures within blood vessels and other bodily compartment is crucial in the diagnosis and management of multiple medical conditions. Presently, techniques for pressure measurement are invasive or have limited accuracy and scope of assessment. Utilizing the subharmonic signal of ultrasound contrast agents offers a promising solution that could address these limitations. After the initial development of this technology in the late nineties, further investigation has brought subharmonic pressure estimation from in vitro exploration to attempts at clinical implementation. However, lack of availability of subharmonic imaging on most clinical scanners, and variability of subharmonic response with different contrast agents have impeded clinical acceptance and widespread use of this modality. This review examines subharmonic imaging and the use of ultrasound contrast agents for estimating physiological pressures, particularly in the heart and portal venous system. A focus is placed on clinically relevant physiologic pressures and their existing measurement approaches, the physics of subharmonic signal generation, in vitro studies demonstrating key findings, and more recent clinical trials. The review also highlights present limitations and future research directions that may help advance clinical translation.

Introduction

Alterations in physiologic pressures are a fundamental aspect in the emergence and evolution of multiple human diseases. In particular, heart failure, cirrhosis, and pulmonary hypertension are complex medical conditions resulting in significant patient mortality and morbidity, as well as considerable healthcare expenditure [1–4]. A shared feature in the physiology of all three of these disease processes is the development of elevated vascular pressures which subsequently results in maladaptive clinical manifestations. Heart failure is defined as a clinical syndrome with symptoms and signs caused by a structural or functional cardiac impairment that leads to pulmonary and systemic vascular congestion [5]. Pulmonary hypertension is a heterogeneous condition marked by an abnormal increase in pulmonary artery pressures, which occurs through a variety of precipitating causes [6]. Broadly, this is due to processes causing increased resistance to flow in the pulmonary circulation, including vascular remodeling, recurrent blood clots, or left-sided heart failure. In both heart failure and pulmonary hypertension, elevated cardiac and pulmonary pressures can cause peripheral edema, progressive ventricular failure, arrhythmias, cardiorenal syndrome, hepatic dysfunction, and respiratory failure [7,8]. Cirrhosis is characterized by progressive liver fibrosis and impaired function due to underlying causes such as alcohol use, hepatitis, autoimmune disease, or metabolic dysfunction-associated steatotic liver disease [9]. With ongoing fibrosis, remodeling of the liver vasculature leads to elevation in pressures in the portal venous system, resulting in variceal bleeding, ascites, peripheral edema, and kidney impairment. Therefore, the measurement of portal vein, cardiac, and pulmonary arterial pressures is important in the diagnosis and management of these diseases. Effective care of other disease processes, such as essential hypertension or disorders associated with elevated intracranial pressure, also relies on knowledge of pressure values. Presently, there are two overall approaches to the assessment of physiologic pressures within the body: direct invasive measurement using a pressure catheter or non-invasive estimation using various modalities, such as ultrasound, pressure cuffs, and impedance devices. However, catheterization carries procedural risks and is costly [10–15],

* Corresponding author. Department of Bioengineering, University of Washington, Seattle, WA, USA.
E-mail address: maverk@uw.edu (M.A. Averkiou).

https://doi.org/10.1016/j.ultrasmedbio.2026.03.027
Received 14 July 2025; Revised 30 March 2026; Accepted 31 March 2026

0301-5629/© 2026 World Federation for Ultrasound in Medicine and Biology. Published by Elsevier Inc.

while current non-invasive technologies have a limited scope of assessment and varying degrees of accuracy [14–20].

A promising technique in addressing these limitations utilizes contrast-enhanced ultrasound (CEUS). Diagnostic ultrasound is a safe, bedside, and low-cost diagnostic imaging modality with a wide variety of clinical applications [21]. Ultrasound has allowed for real-time visualization of multiple organs, vascular structures, soft tissues, body cavities, and joint spaces. A significant advancement in the field of medical ultrasound was the development of microbubble ultrasound contrast agents (UCAs) [22]. CEUS is now regularly used to improve the quality of ultrasound imaging, with left ventricular opacification being one of the most used clinical applications. Unlike the contrast material of other imaging modalities, UCAs are a blood pool agent and provide important information about the macro- and micro-vasculature. The gas-filled microbubbles are encapsulated with a protein or lipid shell, and when exposed to ultrasound, oscillate and generate a nonlinear echo response that can be separated from the linear signal derived from tissue. While conventional CEUS forms images with the nonlinear signal (whole harmonics of the transmit frequency), another approach is to form images with the subharmonic signal (half the transmit frequency) that only microbubbles generate [22,23]. In the late 1990s, the subharmonic signal of UCAs were also investigated for their ability to measure hydrostatic pressure in its surrounding medium. Shi et al. in 1999 demonstrated sensitivity to changes in hydrostatic pressure with commercially available UCAs (shelled microbubbles) [24]. It was shown that the subharmonic component of the echo signal generated from the UCA Levovist decreased linearly with increasing hydrostatic pressure of the surrounding fluid. This relationship became the basis for pressure estimation using UCAs, as they can be delivered to and visualized in nearly any vascular site within the body. This approach, most commonly referred to as subharmonic-aided pressure estimation (SHAPE), has now been further explored through several in vitro studies, animal experiments, and human clinical trials. Despite many investigations, technical limitations such as the need for a secondary device to calibrate subharmonic signal to absolute pressure [25–33], uncertainty surrounding the most effective methodology due to the broad range of acoustic parameters (transmit frequency, pulse length, acoustic pressure) and microbubble formulations, and installation in only a limited number of scanners have impeded clinical acceptance and broad use of this modality.

In this review, we describe the relevant knowledge and literature encompassing subharmonic imaging and the use of the subharmonic signal of UCAs for physiologic pressure estimation, with a particular emphasis on evaluating cardiac and portal vein pressures. First, we review the current guideline-accepted techniques for pressure measurement and non-invasive pressure estimation. We then discuss the physical mechanisms behind subharmonic signal generation from microbubbles, the influence of hydrostatic pressure, and the initial in vitro studies exploring UCA pressure sensitivity. Finally, we highlight recent studies involving early clinical implementation of this technique, limitations of these efforts, and possible areas of future study to advance this technology, all of which may be important for its complete clinical translation and widespread use in medicine. Further, we believe that the multidisciplinary perspective offered, integrating the viewpoints of engineers and physicians, will contribute meaningfully to the development of a clinically relevant approach.

Current methods for physiologic pressure measurement

Cardiopulmonary pressures

Assessment of cardiopulmonary pressures is performed primarily by direct measurement via invasive catheterization or indirect estimation via noninvasive Doppler echocardiography [17,34–36]. During direct/invasive measurement, pressures can be measured in the peripheral arteries via arterial catheterization, in the left heart chambers and central arteries via left heart catheterization (LHC), or in the venous system,

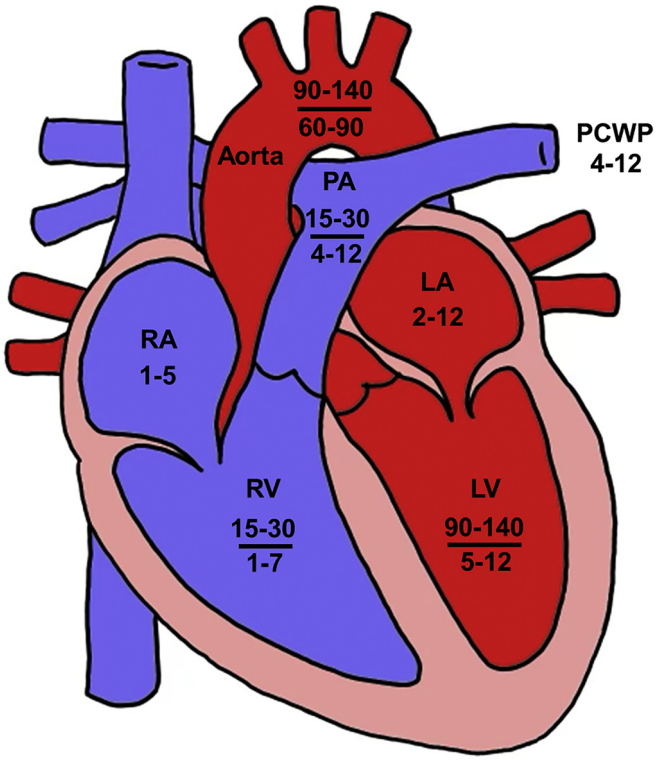


Figure 1. Diagram of the cardiac chambers with respective normal cardiopulmonary pressure ranges in mm Hg. For locations exhibiting significant differences during systole and diastole, the systolic pressure range is placed immediately above the diastolic pressure range. RA, right atrium; RV, right ventricle; LA, left atrium; LV, left ventricle; PA, pulmonary artery; PAWP, pulmonary artery wedge pressure.

right heart chambers, and pulmonary arteries via right heart catheterization (RHC). RHC also provides an estimate of left atrial pressure obtained by "wedging" the inflated catheter into a distal pulmonary artery, allowing pressure equilibration with the left heart and yielding the pulmonary arterial wedge pressure (PAWP) [34]. Figure 1 shows the approximate normal ranges for these values [37]. The mean pulmonary artery pressure (mPAP) and PAWP are of particular importance as they define pulmonary hypertension (mPAP > 20 mm Hg) and identify the presence of impaired left heart function (PAWP > 15 mm Hg) [38]. The full range of pressures encountered in the majority patients with and without disease during the evaluation of the pulmonary arteries and right heart chambers is generally between ~0 and 100 mm Hg [39,40]. RHC is particularly valuable as it is currently required for the diagnosis of pulmonary hypertension, is used in the evaluation of heart failure, and is employed in the intensive care unit to help manage patients with complex forms of shock. LHC is performed similarly, with insertion of a catheter into the femoral artery or radial artery and advancement to the aorta, coronary arteries, and left heart chambers [35]. Both RHC and LHC provide highly accurate pressure measurements but are invasive procedures associated with procedural risks and high costs [10–12].

Doppler echocardiography is non-invasive but provides limited pressure data with only right atrial pressure (RAP) and right ventricular systolic pressure (RVSP) being routinely estimated [36]. Further, as these values are indirectly based on other parameters, they can be inaccurate or cannot be calculated at all if measurements of the underlying parameters are missing. RAP equilibrates with the central veins and is thus approximated using the diameter and degree of collapse of the inferior vena cava (IVC) during a sniff maneuver [36]. Limitations include poor accuracy, provision of pressure ranges rather than a single absolute pressure value, and use of this approach being precluded in certain clinical

scenarios, such as when patients receive positive pressure ventilation. Jugular venous ultrasound has been recently described as another method used to estimate RAP but also suffers from limited accuracy [41]. RVSP is derived through use of the modified Bernoulli equation, which describes the relationship between pressure, kinetic energy, and gravitational potential energy of fluid in an enclosed container [36]. When applied to blood flow in the heart, the Bernoulli equation can be simplified to calculate the pressure change between two different locations as a function of flow velocity. This is specifically applied to determine the pressure gradient between the right atrium and right ventricle, with the flow velocity being the peak tricuspid valve regurgitant velocity (TRV). Continuous wave Doppler is utilized to measure TRV. The estimated pressure differential is then added to the RAP, estimated from IVC measurement, to determine the RVSP, which typically closely approximates pulmonary artery systolic pressure (PASP).

Several studies have also compared RVSP and PASP estimation with the gold standard of RHC measurements. The R-squared value between PASP estimated from echocardiography and RHC has been shown to be 0.49, with echocardiography having a sensitivity of 83% and specificity of 72% in the diagnosis of pulmonary hypertension [19]. Accuracy is further reduced in patients with lung disease [18]. Additionally, absence of detectable tricuspid regurgitation does not necessarily indicate lack of elevated pulmonary artery pressures. One study evaluated patients referred for RHC and found that 36% of patients had had an unmeasurable TRV on echocardiogram, and 53% of those patients were subsequently found to have elevated pulmonary pressures on RHC [42]. For the left heart, echocardiography does have some efficacy in being able to predict left-sided pressure elevation in certain clinical scenarios [43], but is unable to determine the absolute left atrial or left ventricular pressures.

Portal venous pressure

Analogous to cardiac pressure measurement, the reference method for portal pressure requires catheterization [14,44]. A balloon-tipped catheter is inserted in the right internal jugular vein and advanced to the right hepatic vein with fluoroscopic guidance. The free hepatic venous pressure is first recorded, after which the balloon is inflated to occlude the hepatic vein and allow for measurement of the wedged hepatic venous pressure. The free hepatic venous pressure value is then subtracted from the wedged hepatic venous pressure value to determine the hepatic venous pressure gradient (HVPG), which is the accepted surrogate measurement of portal venous pressure. Figure 2 displays a diagram of the hepatic vasculature in normal and cirrhotic liver during HVPG measurement. The normal range for HVPG is 1–5 mm Hg, with elevation beyond 10 mm Hg specifically associated with higher rates of complications and mortality. Therefore, an HVPG value of 10 mm Hg or greater defines clinically significant portal hypertension [14]. The overall range of pressures typically encountered in patients during this procedure is ~0–40 mm Hg [45]. In addition to the invasiveness of the procedure, constraints include high cost and limited availability due to the expertise required; direct measurement of the portal venous pressure is generally not performed as it is even more invasive [14]. There are presently no guideline-accepted indirect methods for absolute portal venous pressure or HVPG measurement [14,16].

Other anatomical pressures

Arterial blood pressure values are most often used in the identification of patients with essential hypertension and for the monitoring of hospitalized patients. Use of a sphygmomanometer to measure arterial blood pressure is sufficient in most circumstances except in the intensive care unit and the operating room where arterial catheterization is required for continuous hemodynamic monitoring [13]. Intracranial pressure (ICP) monitoring is crucial for the management of neurologic processes, such as traumatic brain injury and subarachnoid hemorrhage, as it can identify pathologic elevations that can lead to life-threatening herniation and/or global hypoperfusion [15]. The normal range for ICP is approximately 7–15 mm Hg while values greater than 20 mm Hg are considered to be elevated [15,46]. Invasive evaluation with a ventricular catheter or intraparenchymal transducer is the preferred and most accurate methodology. Intraocular [47], intra-abdominal [48], pleural [49],

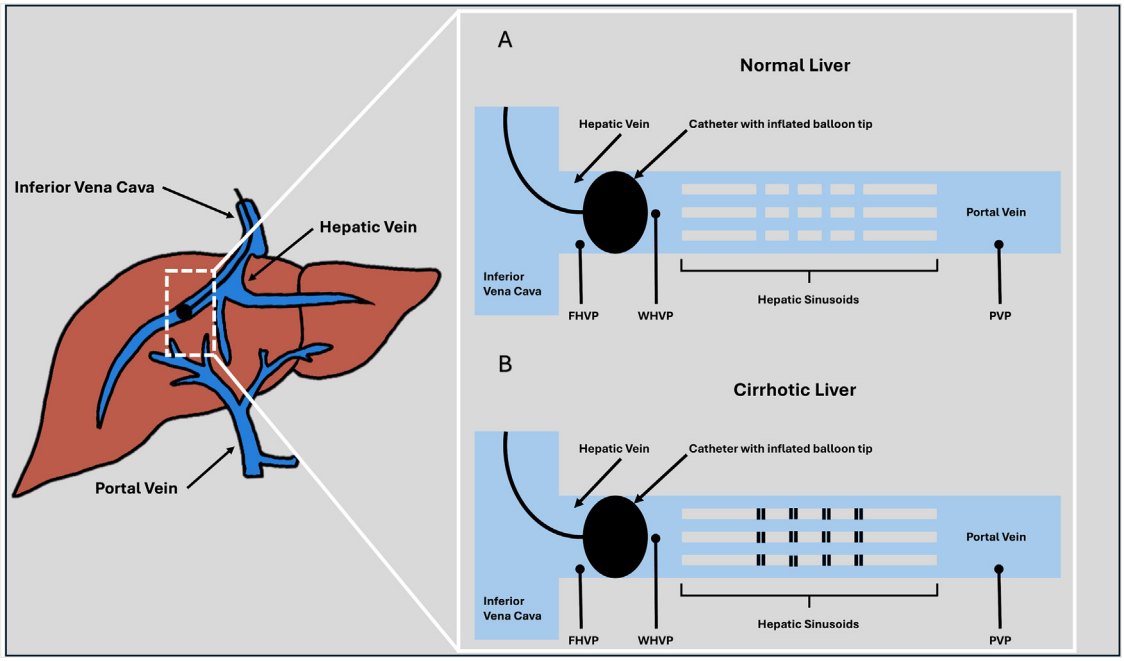


Figure 2. Representation of the measurement of the hepatic venous pressure gradient (HVPG). (a) depicts measurement of the HVPG in normal liver vasculature. After occlusion of blood flow in a hepatic vein with a balloon catheter, the pressure of the static column of blood (the wedged hepatic venous pressure or WHVP) equilibrates with the hepatic sinusoidal pressure. The HVPG is calculated by subtracting the free hepatic venous pressure (FHVP) from the WHVP. (b) illustrates cirrhotic physiology in which fibrosis distorts the sinusoidal vascular architecture. As a result, the WHVP now equilibrates with the portal venous pressure (PVP), thereby allowing the HVPG to be used as surrogate of direct portal vein pressure measurement.

and tissue compartment pressures [50] are also relevant to management of various other disease processes.

Principles of contrast imaging

Subharmonic imaging with UCAs is a technique for noninvasively monitoring pressures and has been a topic of many investigations since the late 1990s. Standard B-mode imaging typically involves the transmission of MHz (2–10 for cardiac, abdominal and peripheral vascular applications and as high as 20–30 for very superficial applications such as dermatology) sound waves and detection of echoes generated by reflection and scattering within tissues. This modality assumes that ultrasound waves propagate through tissue and scatter in a linear fashion, causing the generated echo signal frequency to be the same as the transmitted frequency [22]. However, it was later discovered that ultrasound propagation in tissue is non-linear, and results in wave distortion and production of additional detectable frequencies that are integer multiples ("harmonic frequencies", $n * f_0$) of the initial transmitted frequency ("fundamental frequency", f_0) [51]. Conversely, when low ultrasound acoustic pressures (< 200 kPa) are used, scattering of sound by tissue is primarily a linear process, i.e. no harmonics are generated [22]. This property of ultrasound waves was particularly advantageous in conjunction with the use of UCAs. When UCAs are insonified at similarly low acoustic pressures, they will oscillate nonlinearly and generate a significant signal at both the fundamental and harmonic frequencies. Figure 3a is a schematic generated in MATLAB (MathWorks, Natick, MA) demonstrating an example frequency spectrum of the signal generated by insonified UCAs. For this simple demonstration, a pulse with harmonic and subharmonic components at user specified levels is generated and its spectrum depicted in Figure 3 is calculated. The scattered pressure having harmonics and subharmonic is described by

$$p_{s(t)} = \left\{ \left[\sum_{i}^{N} A_i \sin(\omega_i t + \varphi) \right] + A_{sbhr} \sin(\omega t) \right\} * E(t)$$

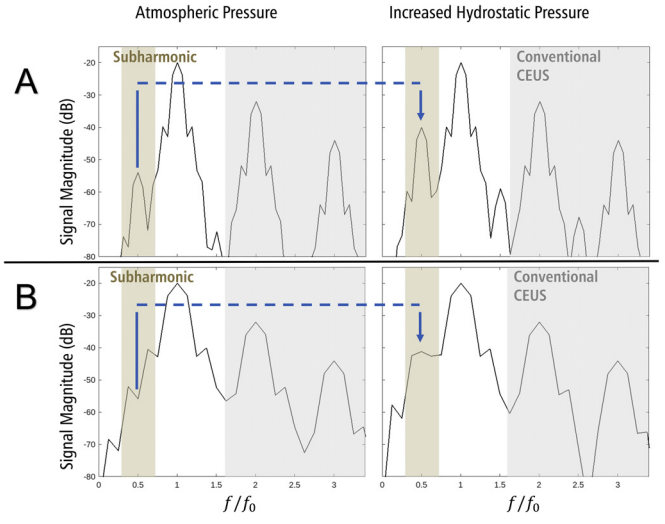


Figure 3. Schematic showing an example of the frequency content of a non-linear 1 MHz pulse scattered from UCAs at atmospheric pressure (left) and at increased pressure (right). The fundamental frequency is at 1 MHz with the subharmonic frequency therefore at 0.5 MHz. With increasing hydrostatic pressure, either a decrease or increase can be seen in the subharmonic signal. In this illustration, the subharmonic signal amplitude increases with an elevation in hydrostatic pressure, while the amplitude of the harmonic frequencies used for conventional CEUS change minimally. Panel A shows the frequency content of an 8-cycle pulse while Panel B shows the frequency content of a 4-cycle pulse. This demonstrates that a reduction in the number of cycles results in broadening and overlap of the signal at the fundamental and subharmonic frequency.

where N is the number of harmonics, A_i are the harmonic amplitudes, A_{sbhr} is the subharmonic amplitude, φ is the phase, ω is the angular frequency, and

$$E(t) = exp\left[-\left(\frac{\omega t}{N_{cyc}\pi} \right)^{2m} \right]$$

is an envelope function with N_{cyc} describing the number of cycles and m the envelope exponent (or slope). As discussed above, because tissues generate minimal harmonic signal at lower acoustic pressures, tuning the ultrasound receiver to the harmonic frequencies will preferentially display the contrast agent [22]. Figure 4 shows examples of the evaluation of the left ventricle and hepatic liver masses with CEUS and standard B-mode imaging. Under certain conditions that vary with different contrast microbubbles, which will be further described in the subsequent section, it is also possible to generate a subharmonic component corresponding to half the transmitted frequency ($f_0/2$). The subharmonic signal, which has been shown to be particularly sensitive to changes in hydrostatic pressure in the surrounding medium, is also illustrated in Figure 3 and can either increase or decrease in magnitude depending on microbubble properties and ultrasound parameters. In the specific example shown here the amplitude of the subharmonic component has increased with hydrostatic pressure but it could also decrease depending on the parameters and contrast agent used. The signal at higher harmonic frequencies detected by conventional CEUS has little to no change in magnitude with increasing hydrostatic pressure. As the subharmonic signal is not produced from tissues, it is possible to generate a subharmonic contrast image whose magnitude is correlated with hydrostatic pressure.

Subharmonic response from UCAs

Early works investigating subharmonic signals from free gas bubbles and encapsulated microbubbles explored the threshold at which these signals are generated at atmospheric pressure and the impact of acoustic conditions such as ultrasound frequency and acoustic pressure. In 1969, Eller and Flynn first described the threshold and frequency dependence of subharmonic generation from free gas bubbles [52]. They found that for subharmonic response an excitation frequency of 2x the resonance was optimal but also that an acoustic pressure above 30 kPa was mandatory. Later, Shankar et al. [53] studied Optison (GE Healthcare, Chicago, IL, USA), a UCA with an albumin shell, and found the threshold for subharmonic signal generation to also be dependent on driving frequency. This threshold was minimized when the driving frequency was twice the average resonance frequency of the microbubble population, with subharmonic signal generated at acoustic pressures as low as 10 kPa in vitro. For off double resonance frequency excitation much high acoustic pressure is mandatory for generating subharmonics. Therefore, there are 2 main mechanisms for subharmonic signal generation: (i) driving the bubble around its resonant frequency which often requires high acoustic pressures (> 200 kPa) to generate a subharmonic component, [54] or (ii) driving the bubble at twice its resonance frequency, where subharmonic signal is detected at low acoustic pressures (< 200 kPa) but is dependent on microbubble shell properties [54–56]. Shi et al [23] also measured subharmonic signal generation with Optison near its resonance frequency, and introduced the development of subharmonic signal generation as a function of acoustic pressure characterized by three stages: "occurrence" where subharmonic signals are minimal, "growth" where the magnitude of the subharmonic signal rapidly increases with acoustic pressure, and "saturation" where subharmonic signal magnitude remains relatively constant despite increasing acoustic pressure. The range of acoustic pressures used in this study (40–250 kPa) slightly exceeds the level at which microbubble shell disruption (detectable signal deterioration in imaging) occurs, which has been estimated to be as low as 200 kPa depending on the microbubble size and driving frequency [54,56]. Transmitting at twice the resonance frequency also

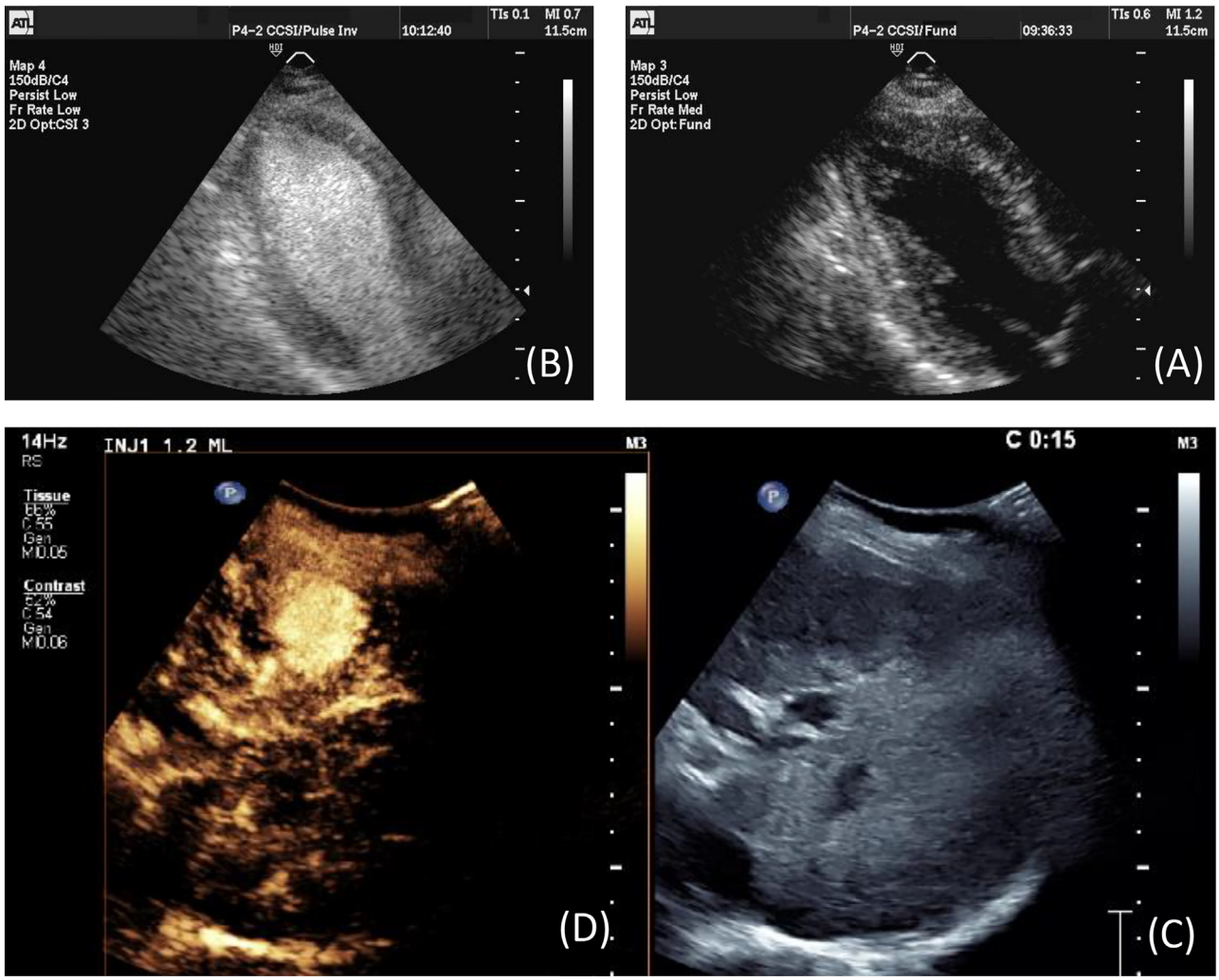


Figure 4. Standard B-mode and CEUS images of the left ventricle and hepatic masses. (a) and (b) are examples of ultrasound images of the left ventricle with B-mode and CEUS respectively. (c) represents a B-mode image of a hepatocellular carcinoma (HCC) while (d) shows its CEUS-image. As demonstrated in these images, the CEUS greatly enhances the visualization of the anatomy of both normal and abnormal structures.

impacts subharmonic behavior as a function of acoustic pressure, as recent in-vitro evaluations of SonoVue (phospholipid shell) observed a different three stage behavior characterized as initial growth (< 300 kPa), saturation (300–400 kPa), and a second growth stage (> 400 kPa) [57,58]. Stable cavitation has been historically associated with the presence of a subharmonic component, where bubbles oscillate around an equilibrium size and can continue for many cycles of continuous acoustic pressure [59], but the reverse statement is not true, that is, a subharmonic component does not always mean stable cavitation. Although a recent publication calls into question the use of frequency content as indicators of cavitation behavior [60], so called stable and inertial cavitation are widely used as a therapeutic tool today for opening of the blood-brain barrier [61] and enhanced systemic drug delivery [62], respectively.

The relationship between subharmonic signal and acoustic pressure led several groups to further investigate the mechanisms behind subharmonic microbubble oscillation. For free/unencapsulated bubbles driven at twice their resonance frequency, the acoustic pressure threshold for subharmonic components is about 30 kPa [52]. Some encapsulated microbubbles at low acoustic pressures (5–100 kPa) driven at twice the resonant frequency exhibit compression-only behavior, which has been confirmed with optical measurements using a high-speed camera [55] and experiments monitoring scattered subharmonic signal [63]. The rapid change in the effective surface tension of the bubble's shell can result in an asymmetric (compression-only) behavior [64] as it transitions from elastic and buckled states, as described by Marmottant et al [65]. The subharmonic behavior of phospholipid-shell microbubbles is primarily driven by these rapid surface tension changes, assuming the microbubble shell is saturated with phospholipids to allow for a large change in shell elasticity to initiate subharmonic behavior. In general, as acoustic pressure increases (> 200 kPa) with long bursts (≥ 8 cycles), microbubble disruption and shell lipid shedding will occur, leaving a free gas bubble and shifting the asymmetry of bubble oscillations to favor expansion behavior [64,65]. These increased pressures also exceed the destruction threshold of certain microbubbles that are resonant at the transmit frequency, indicating that subharmonic signal in this pressure regime is likely due to a combination of the destruction of resonant microbubbles and certain microbubbles oscillating at twice the resonance frequency [54,63]. The work by Chomas et al [54] shows that the subharmonic generation at twice the resonance frequency is dominant below the destruction threshold for microbubbles (for bubble radii > 2 μm, acoustic pressure ≤ 500 kPa), while subharmonic signal from bubbles driven at their resonant frequency are dominant above the destruction threshold (bubble radii ≤ 2 μm, acoustic pressures > 500 kPa). Since UCAs are polydisperse with an average bubble size, transmit frequency and acoustic pressure must be carefully selected for appropriate

subharmonic signal generation. In diagnostic ultrasound, microbubble destruction begins at a mechanical index (MI) of about 0.1, and an MI of 0.3 and above can impair real-time imaging, requiring triggering techniques [66–68].

The dependence of the subharmonic signal on frequency and acoustic pressure holds true at atmospheric pressure, but increasing the hydrostatic pressure introduces new effects on microbubble oscillation that impact subharmonic response. Generally, as hydrostatic pressure increases above atmospheric pressure, 3 major effects should take place: (i) increased compressive force on microbubbles, (ii) increased dissolution rate of free bubbles, and (iii) a shift in resonant frequency [69–71]. Further, the shift in resonance frequency may have two contributions depending on the condition of the microbubble shell: (i) for free gas bubbles (after shell disruption) there is little to no change due to the weak dependence of the resonant frequency on hydrostatic pressure and initial radius, or (ii) shelled microbubbles shifting to a buckled, tensionless shell state with increased hydrostatic pressure. At low acoustic pressures where we only expect compression behavior, only the dissolution rate and resonance shift need be considered, while high acoustic pressures must consider all 3 effects. For microbubbles insonified at low acoustic pressures, an increase in hydrostatic pressure should exaggerate compression behavior and increase the subharmonic signal [55,63,72], as depicted in Figure 3.

In vitro investigations of subharmonic pressure estimation

The initial experiments evaluating the relationship between the subharmonic signal amplitude of UCAs and the hydrostatic pressure of the UCA fluid medium were performed by Shi et al [24]. For this study, Levovist (Schering AG, Berlin, Germany) was placed in a fluid-filled pressure chamber and the subharmonic signal was measured at five different hydrostatic pressure values between 0 and 186 mm Hg using an acoustic pressure of 390 kPa. This acoustic pressure placed Levovist in the "growth" stage and therefore made the subharmonic signal most sensitive to changes in the surrounding environment. The subharmonic signal was recorded at each hydrostatic pressure point with the pressure being held static, and the UCA solution was replaced in between each measurement. Over the hydrostatic pressure range of 0–186 mm Hg, it was found that the subharmonic signal decreased by 9.6 dB and exhibited a negative linear relationship ($r = -0.98$) with hydrostatic pressure. This finding launched efforts to implement this technique to non-invasively measure physiologic pressures at various anatomic sites.

Subsequent in vitro studies have modified parameters that could affect the subharmonic signal, most notable of which were UCA type and acoustic pressure. More recent studies have used current clinically available UCAs such as Sonazoid (GE HealthCare, Oslo, Norway) [25,73–79], SonoVue (Bracco, Milan, Italy) [57,58,70,74,79–87], Definity (Lantheus Medical Imaging, North Billerica, MA, USA) [74,76,79,88], Optison [69,76,79,89] and other experimental UCA formulations [54,63,69,72,75,76,80,90]. In the USA, Optison (cardiac), Definity (cardiac), SonoVue (cardiac and liver) are approved for clinical use [91]. Sonazoid has been approved for liver imaging in Japan, South Korea, Taiwan, China, Denmark, and Norway [91–93]. All Sonazoid-based studies have demonstrated a decrease in the subharmonic signal with increasing hydrostatic pressure (similar to Optison and Definity). However, the sensitivity (dB/mm Hg), the detected change in the subharmonic signal in relation to hydrostatic pressure change, has been quite variable. Table 1 describes the sensitivity values reported in each experimental study and is sub-divided by UCA type. We note that a wide variety of experimental setups and conditions are used throughout these studies, which may impact the reported sensitivities and limit direct comparison of reported results. For Sonazoid in vitro investigations, one group noted the sensitivity to be as low as -0.02 dB/mm Hg [79], while another noted -0.22 dB/mm Hg [76], which is more than 10x more sensitive. Furthermore, Sonazoid has been found to have distinct sensitivity values over different hydrostatic pressure ranges: -0.07 dB/mm Hg over the range of 0–200 mm Hg vs. -0.19 dB/mm Hg over the range of 0–50 mm Hg [74]. This finding suggests that the relationship between the subharmonic signal of Sonazoid and hydrostatic pressure is actually *non-linear* over a broad ambient pressure range (0–200 mm Hg). Several studies also investigated modifying the acoustic pressure to identify the optimal setting for maximal hydrostatic pressure sensitivity. Of note, the optimal acoustic pressure was identified to be at relatively high values (≥ 350 kPa) [25,76]. Dave et al. then developed an incident acoustic output (IAO) algorithm to automatically select the optimal acoustic pressure in real-time to facilitate translation to clinical use [94]. The actual range of possible acoustic pressures implemented with this algorithm is broad (0 to 3.34 MPa) and ensuing studies did not delineate a typical acoustic pressure that is utilized [75,77]. More recently, Mayer et al. described that the average acoustic pressure typically achieved through this algorithm for Sonazoid in vitro was 173.33 and 140 kPa for static or dynamic flow conditions respectively, which is significantly lower than what was noted in initial studies [74]. With Definity, the subharmonic signal also has been consistently noted to decrease with increasing hydrostatic pressure, but varying sensitivity across studies and across different pressure ranges is once again noted [74,76,79,88]. Originally, maximal sensitivity was noted to be present at an acoustic pressure of 350 kPa [76], but more recent work suggests that the optimal pressure sensitivity could be attained at acoustic pressures as low as 90 kPa [74].

Table 1
Maximal sensitivity of the subharmonic signal to change in hydrostatic pressure as measured in different experimental studies

UCA type	Study type	Sensitivity (dB/mm Hg)	Hydrostatic pressure range (mm Hg)	Reference
SonoVue	In vitro	-0.24[a]	20–160	[70]
	In vitro	-0.11[a]	0–180	[87]
	In vitro	0.07	0–90	[74]
		-0.19	140–200	
	In vitro	0.16	0–75	[82]
		-0.16	125–200	
	In vitro	0.16	10–40	[57]
		-0.15[a]	10–40	
	In vitro	-0.11[a]	8–180	[83]
	In vitro	0.08[a,b]	0–188	[84]
		-0.07[a,c]	0–188	
	In vitro	-0.06[a]	0–188	[85]
	In vitro	-0.05	0–188	[58]
	In vitro	0.07	0–60	[86]
	In vitro	-0.06	7–74	[79]
	In vitro	-0.12[a]	10–40	[81]
	In vivo	-0.38[a]	5–35	[81]
Sonazoid	In vitro	-0.09	0–120	[73]
	In vitro	-0.07	10–40	[77]
	In vitro	-0.19	0–50	[74]
		-0.07	0–200	
	In vitro	-0.08	0–78	[75]
	In vitro	-0.03	0–120	[78]
	In vitro	-0.08	0–186	[76]
	In vitro	-0.09	0–120	[25]
	In vitro	-0.03	7–74	[79]
	In vivo	-0.20	15–70	[27]
	In vivo	-0.50	20–125	[28]
	In vivo	-0.69	5–35	[33]
	In vivo	-0.62	5–35	[94]
Definity	In vitro	-0.19	0–50	[74]
		-0.04	0–200	
	In vitro	-0.05	15–74	[88]
	In vitro	-0.07	0–186	[76]
	In vitro	-0.10	7–74	[79]
	In vivo	-0.40	0–40	[29]
		-0.09	0–150	

The UCA type and hydrostatic pressure range for which the sensitivity calculation was performed are also listed as these two factors notably affect the magnitude and directionality of the sensitivity.

[a] High acoustic pressure utilized (>200 kPa).

[b] 1.33 MHz driving frequency.

[c] 4 MHz driving frequency.

Conversely, the subharmonic response of SonoVue has been more challenging to characterize, as its relationship with hydrostatic pressure has been found to vary even more significantly depending on the hydrostatic pressure range and applied acoustic pressure. At lower acoustic pressures (≤ 350 kPa), as hydrostatic pressure is increased, the subharmonic amplitude notably linearly increases over the range of 0 to ~40-75 mm Hg, plateaus, and then linearly decreases over the range of ~100–200 mm Hg [57,58,70,74,82,83,86,87]. At higher acoustic pressures (> 350 kPa), only a linear decrease is observed over the range of 0–200 mm Hg [57,58,70,81,83,85,87]. With the exception of excitation frequency [90], this approximate trend appears to be re-demonstrated across nearly all studies even with variations in other transmit parameters. Similar results have also been observed with an experimental perfluorobutane (C_4F_{10}) phospholipid shell microbubble agent (Bracco Research S.A., Geneva, Switzerland) [63]. As described earlier, it has been proposed that the linear increase in subharmonic signal at low acoustic pressures over the lower hydrostatic pressure range is mainly due to compression-only behavior of the microbubbles [55,64], with the subsequent decrease at higher hydrostatic pressures suspected to be due to bubble destruction [82]. Further, the uniform decrease across the entire physiologic pressure range at higher acoustic pressures is also hypothesized to be due to bubble destruction [83] SonoVue's unique response compared to other commercial UCAs could be due to its distinctive lipid shell and SF_6 gas core that result in compression-only behavior similar to the experimental perfluorobutane (C_4F_{10}) phospholipid-shell microbubbles utilized by Frinking et al [63,74,82].

Since blood is rarely static intravascularly and is often subject to cyclic pressure changes with a minimum pressure greater than 0 mm Hg, experiments were performed to assess the impact of fluid flow and hydrostatic pressure variation on the subharmonic signal. Through the use of a flow phantom and flow pump, it was shown that subharmonic amplitude was still detectable and sensitive to pressure changes even under dynamic flow conditions [76] and periodic hydrostatic pressure changes [25]. Later studies further characterized the effect of these factors. Zhang et al. observed that the subharmonic signal of Sonazoid decreased on average by 0.22 dB per minute under constant hydrostatic pressure (50 mm Hg) and flow (6 cm/s) and that signal amplitude was affected by flow velocity (increased by 0.39 dB per 1 cm/s over the range of 4 to 14 cm/s) [78], but a recent publication calls to question some of these results [95]. Time from preparation of the microbubble suspension also had an impact. Further, Azami et al. found that repeated pressurization-depressurization cycles caused the subharmonic signal generated by SonoVue to decay to the noise baseline, and that this effect was particularly pronounced at higher hydrostatic pressures [58]. Two other notable factors – hematocrit concentration and microbubble concentration – were found to have no significant impact on the subharmonic gradient [77].

Finally, Table 2 highlights the combination of excitation frequency and number of cycles used for subharmonic imaging in each in vitro study listed. In this table, we see that most experiments utilize a wide range of excitation frequencies – below, at, and above the resonance frequency of the corresponding microbubble formulation. It is also striking that the subharmonic signal can be detected even with very low number of cycles (2–4) used in some studies. While axial resolution for imaging is gained by using a lower number of cycles, this conversely causes pulse shortening, which can make individual frequency components difficult to distinguish. The frequency spectra of the scattered sound will exhibit broadening of the signal at the fundamental and subharmonic frequency and eventually even overlap if the number of cycles is sufficiently low. Therefore, even if the signal amplitude around a certain bandwidth of the expected subharmonic frequency is used, this may actually be a representation of the broadened higher amplitude fundamental signal. Figure 3b illustrates this phenomenon using simulated non-linear pulses produced with a smaller number of cycles than that used in Figure 3a. We note that some studies have demonstrated that other frequency components, including the various harmonic components, exhibit a change in magnitude due to increased hydrostatic pressure [24,90]. Therefore, it may still be possible to detect a change in signal magnitude with hydrostatic pressure. When evaluating previous works that do not include a frequency spectrum of the received signal it is not possible to tell which frequency components are directly responding to a change in ambient pressure.

Table 2
Ultrasound transmit parameters utilized in the referenced in vitro experimental studies. Studies that have the same transmit parameters are listed together

UCA type	Excitation frequency (MHz)	Number of cycles	Reference
SonoVue	1.33	64	[83,84,87]
	1.7–7	5–16	[82]
	3	32	[58]
	2.5	4	[74]
	3	32	[80]
	4	64	[83,84,87]
	4	16	[57,81]
	4	32	[85]
	4	8	[86]
	5	12	[70]
	5	N/A	[79]
Sonazoid	2.5	2	[25,73]
	2.5-4	2*	[30]
	2.5	4	[74,75]
	2.5	4*	[77]
	1–6	N/A	[78]
	2.5–6.6	64	[76]
	5	N/A	[79]
	2.5	4	[74]
	2.5–6.6	64	[76]
	2.5-4	2*	[30]
	5	N/A	[79,88]

* Parameter not specified in all listed manuscripts but assumed to be unchanged based on prior studies by the same research group using the same clinical system.

In vivo investigation of subharmonic pressure estimation and clinical applications

Similar to in vitro investigations, many in vivo investigations successfully captured the property of the subharmonic component to correlate with hydrostatic pressure. Table 3 lists the specific ultrasound parameters (frequency and number of cycles) of in vivo studies in similar fashion to Table 2 which was for in vitro studies. We will discuss these studies next in the sections that follow.

Table 3
Ultrasound transmit parameters utilized in the referenced in vivo experimental studies. Studies that have the same transmit parameters are listed together

UCA type	Excitation frequency (MHz)	Number of cycles	Reference
SonoVue	4	16	[81]
Sonazoid	2.5	2	[25]
	2.5	2*	[27,28,32]
	2.5	4	[96,97]
	2.5	2, 3, 4	[33]
	2.5	4, 8, 16	[94]
Definity	2.5	2*	[29]
	3	2*	[31]
	8	N/A	[106]

* Parameter not specified in all listed manuscripts but assumed to be unchanged based on prior studies by the same research group using the same clinical system.

Cardiopulmonary pressures

Forsberg et al. were the first to perform in vivo experimentation by measuring aortic pressures in 2 canines with the subharmonic signal generated from Sonazoid [26]. Separate transmit (4 MHz transmit frequency) and receive transducers (2 MHz receive frequency) at an acoustic pressure of 1.6 MPa were used. The subharmonic signal amplitude decreased by 9 dB as the hydrostatic pressure increased from ~20-60 mm Hg. The variation in the subharmonic signal was fitted to the catheter-based aortic pressure measurements. After this initial fitting, aortic pressures estimated with the subharmonic signal were then compared to catheter-based aortic pressure measurements and found to have a root mean square error <27% based on a sample of 2. Although this was a promising result, due to the absence of an imaging mode with the experimental setup, it required a midline abdominal incision to expose the aorta directly to the transducers.

In 2011, subharmonic imaging modes began to be implemented as research options in clinical ultrasound scanners. Table 4 presents the clinical systems currently known to have (or had) subharmonic imaging capability. Unfortunately, even today most of these are only research options and only the GE LOGIQ E10 has a released subharmonic mode on the C1-6 curvilinear array. As a result, ensuing research in canines required only a single transducer with both transmit and receive capabilities, allowed for visualization of the structures of interest, and did not require invasive placement of the probe [25,27,28,94]. A Sonix RP scanner (BK Medical, Burlington, MA, USA) with PA4-2 phased array probe (2.5 MHz transmit frequency, 1.25 MHz receive frequency, 2 cycles, 3.3 kHz PRF, pulse inversion) was used with Sonazoid to estimate cardiac pressures. We note that the PA4-2 probe has very reduced frequency response at 1.25 MHz and the use of 2 cycles does not allow the separation of the subharmonic and the fundamental. Despite this, the subharmonic signal was found to track pressure changes in both the left [25,27] and right ventricle [28] with low error (< 3.5 mm Hg). However, a conversion factor (mm Hg/dB, inverse of the sensitivity) again had to be determined by performing a regression between the subharmonic amplitude and catheter-based aortic pressure measurements. Notably, the conversion factor differed between each canine, so this step was required in each individual canine before the subharmonic signal could be used to independently determine ventricular pressures with accuracy. The acoustic pressures utilized in these studies were adjusted for each individual canine to elicit optimal pressure sensitivity and ranged from 76 to 897 kPa, which is a very broad range that surpasses the destruction threshold of the commonly utilized UCAs.

Clinical testing in subjects referred for cardiac catheterization was first described in 2017 [29]. The SonixTablet clinical system (BK Medical, Burlington, MA, USA) was instead used, but with the same PA4-2 phased array probe and the transmit and receive frequencies listed above. Three acoustic pressure output settings up to 897 kPa were selected. Cardiac ultrasound examination was performed simultaneously with left and right heart catheterization and a continuous infusion of Definity was administered to facilitate subharmonic imaging. Linear regression between the subharmonic amplitude and initial pressure catheter measurements in the aorta was still required to convert subsequent subharmonic data from the cardiac chambers to actual hydrostatic pressure values. Due to technical limitations (unoptimized acoustic pressure), the correlation between the subharmonic signal and catheter data was highly variable (r = -0.3 to -0.9 for LV, r = -0.3 to -0.6 for RV).

After implementation of an interface that quickly trialed 16 different acoustic outputs (up to 897 kPa) through the previously described IAO algorithm, subsequent studies showed improved correlation (r = -0.77 to -0.84) between the subharmonic data and pressure catheter measurements [30–32]. A SphygmoCor XCEL PWA device (ATCOR Medical, Chicago, IL, USA) was also used to noninvasively calibrate the subharmonic signal amplitude and aortic pressures. However, because aortic pressures measured by the SphygmoCor device were often very different than catheter-based aortic pressure measurements, patients again required invasive catheter measurements to calibrate subharmonic measurements before subharmonic data could be used independently to estimate cardiopulmonary pressures. After calibration, both Definity [31] and Sonazoid [32] were found to have low error (< 5 mm Hg for Definity, < 10 mm Hg for Sonazoid) when compared to catheter-based measurements.

Portal pressures

An induced portal hypertension model in canines was used to initially evaluate the accuracy of subharmonic pressure estimation with Sonazoid in determining portal vein pressures [33]. Here, a Logiq E9 scanner (GE HealthCare, Chicago, IL, USA) with a 4C curved array (2.5 MHz transmit frequency, 1.25 MHz receive frequency, 2–4 cycles, pulse inversion) was employed. Three acoustic pressures were selected (140, 230, and 360 kPa). The subharmonic signal amplitude was compared to portal vein pressure measured through invasive catheterization before and after induction of portal hypertension. The change in portal pressure after induction of portal hypertension was found to have a moderate negative correlation with the change in the subharmonic amplitude ($-0.79 < r < -0.70$). Analogous to the previously described cardiac studies, a fitting process between subharmonic and invasive catheter data was then performed to allow for prediction of portal vein pressures.

Eisenbrey et al. then performed a clinical trial in patients planned for transjugular liver biopsy and HVPG measurements [96]. Following the procedure, the portal and hepatic veins were scanned with subharmonic

Table 4
Clinical systems utilized for subharmonic imaging

Clinical system	Probe	Frequency (MHz)	Number of cycles	Pulse type	Reference
Sonix RP	Phased Array PA4-2	2.5	2	PI	[25,27,28,73]
SonixTablet	Phased Array PA4-2	2.5	2[a]	PI[a]	[29–32]
Logiq 9	Curved Array 4C	2.5	2-16	PI[a]	[33,77,94,96,97]
Logiq E10[b,c]	Curved Array C1-6	2.5	4	AM	[74]
	Curved Array C2-9	5	N/A	N/A	[79,88]
	Curved Array C1-6	N/A	N/A	N/A	[78]
Mindray Resona[d]	N/A	N/A	N/A	N/A	

Associated transmit parameters are also provided. The Sonix and Logiq systems are manufactured by BK Medical (Burlington, MA, USA) and GE HealthCare (Chicago, IL, USA) respectively. The Resona family of scanners (Mindray, Shenzen, China) also have a subharmonic imaging mode [74].

[a] Parameter not specified in all listed manuscripts but assumed to be unchanged based on prior studies by the same research group using the same clinical system.

[b] Other probes used in various studies as research options: RAB6, 9L, RSP6-16, IC5-9, RIC5-9.

[c] The Logiq E10 is also referred to as the E20 is certain regions of the world.

[d] The Mindray offers subharmonic imaging but we could not find any reference or other information on the parameters used.

ultrasound (Logiq E9 scanner with a 4C curved array, 2.5 MHz transmit frequency, 1.25 MHz receive frequency, 4 cycles) using an infusion of Sonazoid. The IAO algorithm was utilized to select acoustic pressure, though the typical acoustic pressures chosen were not described. The difference in subharmonic signal between the portal and hepatic veins was then compared to the obtained HVPG values. It was found that patients with elevated HVPG (> 12 mm Hg) had a higher subharmonic signal difference and that using a specific cutoff value in the difference predicted HVPG > 12 mm Hg with sensitivity of 100% and specificity of 81%. This study protocol was later repeated in a larger cohort of patients (137 in this one versus 45 in the earlier one) and similar results were achieved, though the actual correlation between the subharmonic gradient and the HVPG was more modest (r = 0.68) [97]. Several recently published clinical studies have also found good correlation between subharmonic magnitude and hydrostatic pressure for detecting portal hypertension [98–103].

Other applications

Subharmonic imaging may also be useful in clinical contexts beyond intravascular cardiac and hepatic pressure measurement. While a detailed discussion is beyond the scope of this review, these topics are also of significance. Though less extensive, studies have been conducted to evaluate its ability to assess intracranial [104], bladder [88], tumor interstitial pressure [105–108], and compartment pressures [109] as well. Apart from pressure sensing applications, subharmonic imaging has demonstrated some preliminary success in enhancing the characterization of tumors and masses across multiple anatomical sites, such as the breast [110–112], pancreas [113], prostate [114], and adnexa [115]. Monitoring of tumor treatment response to chemotherapy [108], vasa vasorum imaging [116], and carotid artery and plaque assessment [117,118] have also been explored.

Limitations and future directions

The use of the subharmonic signal for non-invasive pressure estimation certainly shows promise and demonstrates persistent interest based on the described in vitro and clinical studies. However, there are several issues that need to be addressed before effective clinical translation. As outlined in this review, there is a very wide range of values noted for the subharmonic signal sensitivity, so clarity on why this degree of variability exists is needed. All clinically approved UCAs (SonoVue, Sonazoid, Definity, and Optison) show differing sensitivity to hydrostatic pressure behavior depending on the range of hydrostatic pressures examined and the acoustic pressures utilized. Although this heterogeneity could be in part be due to differing transmit parameters and experimental design, we believe that a closer examination of whether UCA selection and preparation/delivery methods, specific signal processing, and bubble destruction may be contributing is warranted. A number of studies have used acoustic pressure values that are above the bubble destruction threshold while other experiments have used very few (2–4) cycles for subharmonic imaging, which can make it difficult to separate the subharmonic signal from the fundamental signal. The widely used method of identifying the acoustic pressure that induces the largest change in the subharmonic signal (the "growth" stage) could also result in a range of high acoustic pressures that exceed the acoustic pressure threshold for microbubble shell disruption (> 200 kPa). Further, all pre-clinical and clinical research efforts have adopted the use of continuous microbubble infusion rather than a bolus strategy. We note that the use of a continuous infusion of microbubble UCAs adds a degree of complexity in a clinical environment. Albeit continuous infusion enables longer data acquisition, bubble concentration may fluctuate depending on the patient's cardiac output, and high microbubble concentration can result in acoustic shadowing. To help broaden clinical utility of the microbubble response to hydrostatic pressure changes, subharmonic imaging techniques compatible with bolus injections should be investigated. Many studies have also evaluated the efficacy of this technique over the 0–200 mm Hg pressure range. A greater emphasis should be placed on optimizing the estimation of pressures < 100 mm Hg, and particularly < 50 mm Hg, ranges with more physiologic importance. The normal ranges of right-sided cardiopulmonary pressures shown in Figure 1 do not exceed 30 mm Hg [37]. Even in patients with pulmonary hypertension, right-sided pressures generally are below ~100 mm Hg as discussed previously [39,40]. Diagnosis of pulmonary hypertension and portal hypertension utilize a pressure cutoff of mPAP > 20 mm Hg and HVPG > 5 mm Hg respectively as well [14,38]. Therefore, accuracy in this pressure range could allow for improved non-invasive diagnostic capabilities.

Another key challenge with clinical implementation is the need to initially calibrate the subharmonic signal amplitude with known hydrostatic pressure values at or near the site of interest before absolute pressure can be calculated. This needs to be done in each patient and every time the patient is scanned as the individual characteristics of each patient impacts the conversion between subharmonic signal to hydrostatic pressure. For example, to perform cardiac pressure measurement, the aortic systolic and diastolic pressures were utilized to calculate the conversion factor (mm Hg/dB) in current studies [31,32]. However, aortic pressures cannot yet be attained reliably with a non-invasive approach and still require initial catheterization. Ultimately, this impacts the main potential advantage of this technique, which is *non-invasive* pressure estimation. Further refinement of non-invasive measurements acquired by the SphygmoCor XCEL device could certainly address this issue. While not yet attempted in vivo, an alternative solution offered by Spiekhout et al. is the use of low frequency (~50 kHz) signal that modulates hydrostatic pressure to a pre-determined extent. The degree of change in subharmonic signal with this pressure modulation can then be used for calibration, thereby allowing subsequently detected shifts in the signal amplitude to estimate hydrostatic pressure changes [86]. Even when only the magnitude of pressure change can be determined rather than the absolute pressure values, identifying pressure differentials between adjacent locations alone could be valuable. The difference in subharmonic signal between two adjacent sites could instead be used as a surrogate to prognosticate certain clinical states, which is what is already being proposed for the prediction of elevated portal venous pressures [96,97]. For intra-cardiac pressures, as pulmonary hypertension worsens, the difference in pressure between the left and right ventricles decreases while the pressure difference between the right ventricle and right atrium increases. It is plausible that the subharmonic signal difference or ratio between two of these sites would also change and could then suggest development of the disease. As this method does not rely on the presence of tricuspid regurgitation, it could be of particular use in those patients to supplement current echocardiographic techniques. Recent advances in the production of microbubbles may also offer custom-tailored bubble formulations specifically for non-invasive pressure estimation with subharmonic imaging. Efforts into developing monodisperse microbubbles are currently ongoing, offering a smaller size distribution to maximize subharmonic signal, and shell properties compatible with being driven at twice the resonance frequency [75,119]. Overall, we remain optimistic that continued investigation will identify potential solutions and eventually allow for effective and widespread clinical use.

Conflict of interest

The authors have no conflicts of interest to declare.

Acknowledgments

This publication was supported by the National Institute of Biomedical Imaging and Bioengineering of the National Institutes of Health under award number R01EB032655.

References

[1] Savarese G, Becher PM, Lund LH, Seferovic P, Rosano GMC, Coats AJS. Global burden of heart failure: a comprehensive and updated review of epidemiology. Cardiovasc Res 2023;118(17):3272–87. doi: 10.1093/cvr/cvac013.

[2] Devarbhavi H, Asrani SK, Arab JP, Nartey YA, Pose E, Kamath PS. Global burden of liver disease: 2023 update. J Hepatol 2023;79(2):516–37. doi: 10.1016/j.jhep.2023.03.017.

[3] Leary PJ LM, Johnson CO, Emmons-Bell S, Rich S, Corris PA, DuBrock HM, et al. Global, regional, and national burden of pulmonary arterial hypertension, 1990-2021: a systematic analysis for the Global Burden of Disease Study 2021. Lancet Respir Med 2025;13(1):69–79. doi: 10.1016/s2213-2600(24)00295-9.

[4] Watzker A, Alsumali A, Ferro C, Dieguez G, Park C, Lautsch D, et al. Economic burden associated with pulmonary arterial hypertension in the United States. Pharmacoeconomics 2025;43(1):83–91. doi: 10.1007/s40273-024-01427-2.

[5] Bozkurt B, Coats AJS, Tsutsui H, Abdelhamid CM, Adamopoulos S, Albert N, et al. Universal definition and classification of heart failure: a report of the Heart Failure Society of America, Heart Failure Association of the European Society of Cardiology, Japanese Heart Failure Society and Writing Committee of the Universal Definition of Heart Failure: Endorsed by the Canadian Heart Failure Society, Heart Failure Association of India, Cardiac Society of Australia and New Zealand, and Chinese Heart Failure Association. Eur J Heart Fail 2021;23(3):352–80. doi: 10.1002/ejhf.2115.

[6] Bousseau S, Sobrano Fais R, Gu S, Frump A, Lahm T. Pathophysiology and new advances in pulmonary hypertension. BMJ Med 2023;2(1):e000137. doi: 10.1136/bmjmed-2022-000137.

[7] Rosenkranz S, Howard LS, Gomberg-Maitland M, Hoeper MM. Systemic consequences of pulmonary hypertension and right-sided heart failure. Circulation 2020;141(8):678–93. doi: 10.1161/circulationaha.116.022362.

[8] Arrigo M, Jessup M, Mullens W, Reza N, Shah AM, Sliwa K, et al. Acute heart failure. Nat Rev Dis Primers 2020;6(1):16. doi: 10.1038/s41572-020-0151-7.

[9] Ginès P, Krag A, Abraldes JG, Solà E, Fabrellas N, Kamath PS. Liver cirrhosis. Lancet 2021;398(10308):1359–76. doi: 10.1016/s0140-6736(21)01374-x.

[10] Chen Y, Shlofmitz E, Khalid N, Bernardo NL, Ben-Dor I, Weintraub WS, et al. Right heart catheterization-related complications: a review of the literature and best practices. Cardiol Rev 2020;28(1):36–41. doi: 10.1097/crd.0000000000000270.

[11] Al-Hijji MA, Lennon RJ, Gulati R, El Sabbagh A, Park JY, Crusan D, et al. Safety and risk of major complications with diagnostic cardiac catheterization. Circ Cardiovasc Interv 2019;12(7):e007791. doi: 10.1161/circinterventions.119.007791.

[12] Oseran AS, Ati S, Feldman WB, Gondi S, Yeh RW, Wadhera RK. Assessment of prices for cardiovascular tests and procedures at top-ranked US hospitals. JAMA Intern Med 2022;182(9):996–9. doi: 10.1001/jamainternmed.2022.2602.

[13] Scheer B, Perel A, Pfeiffer UJ. Clinical review: complications and risk factors of peripheral arterial catheters used for haemodynamic monitoring in anaesthesia and intensive care medicine. Crit Care 2002;6(3):199–204. doi: 10.1186/cc1489.

[14] Kaplan DE, Ripoll C, Thiele M, Fortune BE, Simonetto DA, Garcia-Tsao G, et al. AASLD Practice Guidance on risk stratification and management of portal hypertension and varices in cirrhosis. Hepatology 2024;79(5):1180–211. doi: 10.1097/hep.0000000000000647.

[15] Hawryluk GWJ, Citerio G, Hutchinson P, Kolias A, Meyfroidt G, Robba C, et al. Intracranial pressure: current perspectives on physiology and monitoring. Intensive Care Med 2022;48(10):1471–81. doi: 10.1007/s00134-022-06786-y.

[16] Hai Y, Chong W, Eisenbrey JR, Forsberg F. Network meta-analysis: noninvasive imaging modalities for identifying clinically significant portal hypertension. Dig Dis Sci 2022;67(7):3313–26. doi: 10.1007/s10620-021-07168-y.

[17] Parasuraman S, Walker S, Loudon BL, Gollop ND, Wilson AM, Lowery C, et al. Assessment of pulmonary artery pressure by echocardiography-a comprehensive review. Int J Cardiol Heart Vasc 2016;12:45–51. doi: 10.1016/j.ijcha.2016.05.011.

[18] Ni JR, Yan PJ, Liu SD, Hu Y, Yang KH, Song B, et al. Diagnostic accuracy of transthoracic echocardiography for pulmonary hypertension: a systematic review and meta-analysis. BMJ Open 2019;9(12):e033084. doi: 10.1136/bmjopen-2019-033084.

[19] Janda S, Shahidi N, Gin K, Swiston J. Diagnostic accuracy of echocardiography for pulmonary hypertension: a systematic review and meta-analysis. Heart 2011;97(8):612–22. doi: 10.1136/hrt.2010.212084.

[20] Amoore JN. Oscillometric sphygmomanometers: a critical appraisal of current technology. Blood Press Monit 2012;17(2):80–8. doi: 10.1097/MBP.0b013e32835026b0.

[21] Rajamani A, Arun Bharadwaj P, Hariharan S, Ragavan AV, Hassan A, Arvind H, et al. A historical timeline of the development and evolution of medical diagnostic ultrasonography. J Clin Ultrasound 2024;52(9):1419–37. doi: 10.1002/jcu.23808.

[22] Averkiou MA, Bruce MF, Powers JE, Sheeran PS, Burns PN. Imaging methods for ultrasound contrast agents. Ultrasound Med Biol 2020;46(3):498–517. doi: 10.1016/j.ultrasmedbio.2019.11.004.

[23] Shi WT, Forsberg F, Hall AL, Chiao RY, Liu JB, Miller S, et al. Subharmonic imaging with microbubble contrast agents: initial results. Ultrason Imaging 1999;21(2):79–94. doi: 10.1177/016173469902100201.

[24] Shi WT, Forsberg F, Raichlen JS, Needleman L, Goldberg BB. Pressure dependence of subharmonic signals from contrast microbubbles. Ultrasound Med Biol 1999;25(2):275–83. doi: 10.1016/s0301-5629(98)00163-x.

[25] Dave JK, Halldorsdottir VG, Eisenbrey JR, Liu JB, McDonald ME, Dickie K, et al. Noninvasive estimation of dynamic pressures in vitro and in vivo using the subharmonic response from microbubbles. IEEE Trans Ultrason Ferroelectr Freq Control 2011;58(10):2056–66. doi: 10.1109/tuffc.2011.2056.

[26] Forsberg F, Liu JB, Shi WT, Furuse J, Shimizu M, Goldberg BB. In vivo pressure estimation using subharmonic contrast microbubble signals: proof of concept. IEEE Trans Ultrason Ferroelectr Freq Control 2005;52(4):581–3. doi: 10.1109/tuffc.2005.1428040.

[27] Dave JK, Halldorsdottir VG, Eisenbrey JR, Raichlen JS, Liu JB, McDonald ME, et al. Noninvasive LV pressure estimation using subharmonic emissions from microbubbles. JACC Cardiovasc Imaging 2012;5(1):87–92. doi: 10.1016/j.jcmg.2011.08.017.

[28] Dave JK, Halldorsdottir VG, Eisenbrey JR, Raichlen JS, Liu JB, McDonald ME, et al. Subharmonic microbubble emissions for noninvasively tracking right ventricular pressures. Am J Physiol Heart Circ Physiol 2012;303(1):H126–32. doi: 10.1152/ajpheart.00560.2011.

[29] Dave JK, Kulkarni SV, Pangaonkar PP, Stanczak M, McDonald ME, Cohen IS, et al. Non-invasive intra-cardiac pressure measurements using subharmonic-aided pressure estimation: proof of concept in humans. Ultrasound Med Biol 2017;43(11):2718–24. doi: 10.1016/j.ultrasmedbio.2017.07.009.

[30] Esposito C, Dickie K, Forsberg F, Dave JK. Developing an interface and investigating optimal parameters for real-time intracardiac subharmonic-aided pressure estimation. IEEE Trans Ultrason Ferroelectr Freq Control 2021;68(3):579–85. doi: 10.1109/tuffc.2020.3016264.

[31] Esposito C, Machado P, McDonald ME, Savage MP, Fischman D, Mehrotra P, et al. Noninvasive evaluation of cardiac chamber pressures using subharmonic-aided pressure estimation with definity microbubbles. JACC Cardiovasc Imaging 2023;16(2):224–35. doi: 10.1016/j.jcmg.2022.09.013.

[32] Esposito C, Machado P, McDonald ME, Savage MP, Fischman D, Mehrotra P, et al. Evaluation of intracardiac pressures using subharmonic-aided pressure estimation with sonazoid microbubbles. Radiol Cardiothorac Imaging 2024;6(1):e230153. doi: 10.1148/ryct.230153.

[33] Dave JK, Halldorsdottir VG, Eisenbrey JR, Merton DA, Liu JB, Zhou JH, et al. Investigating the efficacy of subharmonic aided pressure estimation for portal vein pressures and portal hypertension monitoring. Ultrasound Med Biol 2012;38(10):1784–98. doi: 10.1016/j.ultrasmedbio.2012.06.013.

[34] Callan P, Clark AL. Right heart catheterisation: indications and interpretation. Heart 2016;102(2):147–57. doi: 10.1136/heartjnl-2015-307786.

[35] Archbold RA, Robinson NM, Schilling RJ. Radial artery access for coronary angiography and percutaneous coronary intervention. Bmj 2004;329(7463):443–6. doi: 10.1136/bmj.329.7463.443.

[36] Mukherjee M, Rudski LG, Addetia K, Afilalo J, D'Alto M, Freed BH, et al. Guidelines for the echocardiographic assessment of the right heart in adults and special considerations in pulmonary hypertension: recommendations from the American Society of Echocardiography. J Am Soc Echocardiogr 2025;38(3):141–86. doi: 10.1016/j.echo.2025.01.006.

[37] Libby P, Bonow RO, Mann DL, Tomaselli GF, Bhatt DL, Braunwald E, Solomon SD. Braunwald's heart disease: a textbook of cardiovascular medicine. Philadelphia, US: Elsevier; 2021.

[38] Humbert M, Kovacs G, Hoeper MM, Badagliacca R, Berger RMF, Brida M, et al. 2022 ESC/ERS Guidelines for the diagnosis and treatment of pulmonary hypertension. Eur Heart J 2022;43(38):3618–731. doi: 10.1093/eurheartj/ehac237.

[39] Farber HW, Foreman AJ, Miller DP, McGoon MD. REVEAL Registry: correlation of right heart catheterization and echocardiography in patients with pulmonary arterial hypertension. Congest Heart Fail 2011;17(2):56–64. doi: 10.1111/j.1751-7133.2010.00202.x.

[40] McGoon MD, Miller DP. REVEAL: a contemporary US pulmonary arterial hypertension registry. Eur Respir Rev 2012;21(123):8–18. doi: 10.1183/09059180.00008211.

[41] Istrail L, Kiernan J, Stepanova M. A novel method for estimating right atrial pressure with point-of-care ultrasound. J Am Soc Echocardiogr 2023;36(3):278–83. doi: 10.1016/j.echo.2022.12.008.

[42] O'Leary JM, Assad TR, Xu M, Farber-Eger E, Wells QS, Hemnes AR, et al. Lack of a tricuspid regurgitation doppler signal and pulmonary hypertension by invasive measurement. J Am Heart Assoc 2018;7(13):e009362. doi: 10.1161/jaha.118.009362.

[43] Andersen OS, Smiseth OA, Dokainish H, Abudiab MM, Schutt RC, Kumar A, et al. Estimating left ventricular filling pressure by echocardiography. J Am Coll Cardiol 2017;69(15):1937–48. doi: 10.1016/j.jacc.2017.01.058.

[44] Lu Q, Leong S, Lee KA, Patel A, Chua JME, Venkatanarasimha N, et al. Hepatic venous-portal gradient (HVPG) measurement: pearls and pitfalls. Br J Radiol 2021;94(1124):20210061. doi: 10.1259/bjr.20210061.

[45] Moitinho E, Escorsell A, Bandi JC, Salmerón JM, García-Pagán JC, Rodés J, et al. Prognostic value of early measurements of portal pressure in acute variceal bleeding. Gastroenterology 1999;117(3):626–31. doi: 10.1016/s0016-5085(99)70455-5.

[46] Albeck MJ, Børgesen SE, Gjerris F, Schmidt JF. Sørensen PS. Intracranial pressure and cerebrospinal fluid outflow conductance in healthy subjects. J Neurosurg 1991;74(4):597–600. doi: 10.3171/jns.1991.74.4.0597.

[47] Da Silva F, Lira M. Intraocular pressure measurement: a review. Surv Ophthalmol 2022;67(5):1319–31. doi: 10.1016/j.survophthal.2022.03.001.

[48] Li Z, Wang H, Lu F. The development, feasibility and credibility of intra-abdominal pressure measurement techniques: a scoping review. PLoS One 2024;19(3):e0297982. doi: 10.1371/journal.pone.0297982.

[49] Lee HJ, Yarmus L, Kidd D, Amador RO, Akulian J, Gilbert C, et al. Comparison of pleural pressure measuring instruments. Chest 2014;146(4):1007–12. doi: 10.1378/chest.13-3004.

[50] Hammerberg EM, Whitesides Jr. TE, Seiler 3rd JG. The reliability of measurement of tissue pressure in compartment syndrome. J Orthop Trauma 2012;26(1):24–31 discussion 2. doi: 10.1097/BOT.0b013e31822908cf.

[51] A new imaging technique based on the nonlinear properties of tissues. In: Averkiou MA, Roundhill DN, Powers JE, editors. 1997 IEEE Ultrasonics Symposium Proceedings An International Symposium (Cat No 97CH36118). IEEE; 1997.

[52] Eller A, Flynn HG. Generation of subharmonics of order one-half by bubbles in a sound field. J Acoust Soc Am 1969;46(3B):722. doi: 10.1121/1.1911753.

[53] Shankar PM, Krishna PD, Newhouse VL. Subharmonic backscattering from ultrasound contrast agents. J Acoust Soc Am 1999;106(4):2104–10 Pt 1. doi: 10.1121/1.428142.
[54] Chomas J, Dayton P, May D, Ferrara K. Nondestructive subharmonic imaging. IEEE Trans Ultrason Ferroelectr Freq Control 2002;49(7):883–92. doi: 10.1109/tuffc.2002.1020158.
[55] de Jong N, Emmer M, Chin CT, Bouakaz A, Mastik F, Lohse D, et al. Compression-only" behavior of phospholipid-coated contrast bubbles. Ultrasound Med Biol 2007;33(4):653–6. doi: 10.1016/j.ultrasmedbio.2006.09.016.
[56] Frinking PJA, de Jong N, Céspedes EI. Scattering properties of encapsulated gas bubbles at high ultrasound pressures. J Acoust Soc Am 1999;105(3):1989–96. doi: 10.1121/1.426732.
[57] Xu G, Lu H, Yang H, Li D, Liu R, Su M, et al. Subharmonic scattering of sonovue microbubbles within 10-40-mmHg overpressures in vitro. IEEE Trans Ultrason Ferroelectr Freq Control 2021;68(12):3583–91. doi: 10.1109/tuffc.2021.3101694.
[58] Azami RH, Forsberg F, Eisenbrey JR, Sarkar K. Acoustic response and ambient pressure sensitivity characterization of SonoVue for noninvasive pressure estimation. J Acoust Soc Am 2024;155(4):2636–45. doi: 10.1121/10.0025690.
[59] Neppiras EA. Acoustic cavitation. Physics Rep 1980;61(3):159–251. doi: 10.1016/0370-1573(80)90115-5.
[60] Wu Q, Gray M, Smith CAB, Bau L, Cleveland RO, Coussios C, Stride E. Challenges in classifying cavitation: correlating high-speed optical imaging and passive acoustic mapping of cavitation dynamics. J Acoust Soc Am 2024;156(5):3608–20. doi: 10.1121/10.0034426.
[61] Sun T, Samiotaki G, Wang S, Acosta C, Chen CC, Konofagou EE. Acoustic cavitation-based monitoring of the reversibility and permeability of ultrasound-induced blood-brain barrier opening. Phys Med Biol 2015;60(23):9079–94. doi: 10.1088/0031-9155/60/23/9079.
[62] Coussios CC, Roy RA. Applications of acoustics and cavitation to noninvasive therapy and drug delivery. Annu Rev Fluid Mech 2008;40(1):395–420. doi: 10.1146/annurev.fluid.40.111406.102116.
[63] Frinking PJ, Brochot J, Arditi M. Subharmonic scattering of phospholipid-shell microbubbles at low acoustic pressure amplitudes. IEEE Trans Ultrason Ferroelectr Freq Control 2010;57(8):1762–71. doi: 10.1109/tuffc.2010.1614.
[64] Sijl J, Dollet B, Overvelde M, Garbin V, Rozendal T, de Jong N, et al. Subharmonic behavior of phospholipid-coated ultrasound contrast agent microbubbles. J Acoust Soc Am 2010;128(5):3239–52. doi: 10.1121/1.3493443.
[65] Marmottant P, van der Meer S, Emmer M, Versluis M, de Jong N, Hilgenfeldt S, Lohse D. A model for large amplitude oscillations of coated bubbles accounting for buckling and rupture. J Acoust Soc Am 2005;118(6):3499–505. doi: 10.1121/1.2109427.
[66] Porter TR, Xie F, Li S, D'Sa A, Rafter P. Increased ultrasound contrast and decreased microbubble destruction rates with triggered ultrasound imaging. J Am Soc Echocardiogr 1996;9(5):599–605. doi: 10.1016/s0894-7317(96)90054-1.
[67] Dietrich C, Ignee A, Hocke M, Schreiber-Dietrich D, Greis C. Pitfalls and artefacts using contrast enhanced ultrasound. Zeitschrift für Gastroenterologie 2011;49(03):350–6.
[68] Fetzer DT, Vijay K, Caserta MP, Patterson-Lachowicz A, Dahiya N, Rodgers SK. Artifacts and technical considerations at contrast-enhanced US. Radiographics 2022;43(2):e220093.
[69] Tremblay-Darveau C, Williams R, Burns PN. Measuring absolute blood pressure using microbubbles. Ultrasound Med Biol 2014;40(4):775–87. doi: 10.1016/j.ultrasmedbio.2013.10.017.
[70] Qiao X, Wen Y, Yu J, Bouakaz A, Zong Y, Wan M. Noninvasive pressure estimation based on the subharmonic response of sonovue: application to intracranial blood pressure assessment. IEEE Trans Ultrason Ferroelectr Freq Control 2022;69(3):957–66. doi: 10.1109/tuffc.2021.3138100.
[71] Bouakaz A, Frinking PJ, de Jong N, Bom N. Noninvasive measurement of the hydrostatic pressure in a fluid-filled cavity based on the disappearance time of micrometer-sized free gas bubbles. Ultrasound Med Biol 1999;25(9):1407–15. doi: 10.1016/s0301-5629(99)00109-x.
[72] Faez T, Renaud G, Defontaine M, Calle S, de Jong N. Dynamic manipulation of the subharmonic scattering of phospholipid-coated microbubbles. Phys Med Biol 2011;56(19):6459–73. doi: 10.1088/0031-9155/56/19/018.
[73] Dave JK, Halldorsdottir VG, Eisenbrey JR, Forsberg F. Processing of subharmonic signals from ultrasound contrast agents to determine ambient pressures. Ultrason Imaging 2012;34(2):81–92. doi: 10.1177/016173461203400202.
[74] Mayer H, Kim GW, Machado P, Eisenbrey JR, Vu T, Wallace K, Forsberg F. Investigation into the subharmonic response of three contrast agents in static and dynamic flow environments using a commercially available diagnostic ultrasound scanner. Ultrasound Med Biol 2024;50(11):1731–8. doi: 10.1016/j.ultrasmedbio.2024.07.015.
[75] van Hoeve W, de Vargas Serrano M, Te Winkel L, Forsberg F, Dave JK, Sarkar K, et al. Improved sensitivity of ultrasound-based subharmonic aided pressure estimation using monodisperse microbubbles. J Ultrasound Med 2022;41(7):1781–9. doi: 10.1002/jum.15861.
[76] Halldorsdottir VG, Dave JK, Leodore LM, Eisenbrey JR, Park S, Hall AL, et al. Subharmonic contrast microbubble signals for noninvasive pressure estimation under static and dynamic flow conditions. Ultrason Imaging 2011;33(3):153–64. doi: 10.1177/016173461103300301.
[77] Gupta I, Eisenbrey JR, Machado P, Stanczak M, Wallace K, Forsberg F. On factors affecting subharmonic-aided pressure estimation (SHAPE). Ultrason Imaging 2019;41(1):35–48. doi: 10.1177/0161734618812083.
[78] Zhang L, Dong YF, Chen Y, Li XG, Wang YH, Wang Y, et al. Impact of microbubble degradation and flow velocity on subharmonic-aided pressure estimation (SHAPE): an experimental investigation. Ultrasound Med Biol 2024;50(7):1020–7. doi: 10.1016/j.ultrasmedbio.2024.03.010.
[79] Kalayeh K, Fowlkes JB, Yeras S, Chen A, Daignault-Newton S, et al. A comparative study of commercially available ultrasound contrast agents for sub-harmonic-aided pressure estimation (SHAPE) in a bladder phantom. Ultrasound Med Biol 2024;50(10):1494–505. doi: 10.1016/j.ultrasmedbio.2024.05.019.
[80] Azami RH, Yapar M, Halder S, Forsberg F, Eisenbrey JR, Sarkar K. Effects of different gas cores on the ambient pressure sensitivity of the subharmonic response of SonoVue. Ultrasound Med Biol 2025;51(2):373–80. doi: 10.1016/j.ultrasmedbio.2024.11.006.
[81] Xu G, Wang Y, Lu H, Li C, Huang L, Su M, et al. Portal vein pressure estimation and portal hypertension discrimination based on subharmonic scattering of ultrasound contrast agent microbubbles. IEEE Trans Biomed Eng 2024;71(1):150–9. doi: 10.1109/tbme.2023.3293952.
[82] Nio AQX, Faraci A, Christensen-Jeffries K, Raymond JL, Monaghan MJ, Fuster D, et al. Optimal control of SonoVue microbubbles to estimate hydrostatic pressure. IEEE Trans Ultrason Ferroelectr Freq Control 2020;67(3):557–67. doi: 10.1109/tuffc.2019.2948759.
[83] Li F, Li D, Yan F. Improvement of detection sensitivity of microbubbles as sensors to detect ambient pressure. Sensors (Basel) 2018;18(12). doi: 10.3390/s18124083.
[84] Sun T, Jia N, Zhang D, Xu D. Ambient pressure dependence of the ultra-harmonic response from contrast microbubbles. J Acoust Soc Am 2012;131(6):4358–64. doi: 10.1121/1.4707512.
[85] Andersen KS, Jensen JA. Impact of acoustic pressure on ambient pressure estimation using ultrasound contrast agent. Ultrasonics 2010;50(2):294–9. doi: 10.1016/j.ultras.2009.09.016.
[86] Spiekhout S, Voorneveld J, de Jong N, Bosch JG. Dual-frequency subharmonic ultrasound contrast imaging for non-invasive blood pressure measurement. Ultrasound Med Biol 2025;51(5):870–6. doi: 10.1016/j.ultrasmedbio.2025.01.015.
[87] Enhanced ambient pressure sensitivity of the subharmonic signal from ultrasound contrast microbubbles. In: Li F, Cai F, Meng L, Jin Q, Zhen H, Li D, editors. 2013 IEEE International Ultrasonics Symposium (IUS); 2013. 21-25 July 2013.
[88] Kalayeh K, Fowlkes JB, Chen A, Yeras S, Fabiilli ML, Claflin J, et al. Pressure measurement in a bladder phantom using contrast-enhanced ultrasonography-a path to a catheter-free voiding cystometrogram. Invest Radiol 2023;58(3):181–9. doi: 10.1097/rli.0000000000000919.
[89] Adam D, Sapunar M, Burla E. On the relationship between encapsulated ultrasound contrast agent and pressure. Ultrasound Med Biol 2005;31(5):673–86. doi: 10.1016/j.ultrasmedbio.2005.01.005.
[90] Azami RH, Forsberg F, Eisenbrey JR, Sarkar K. Ambient pressure sensitivity of the subharmonic response of coated microbubbles: effects of acoustic excitation parameters. Ultrasound Med Biol 2023;49(7):1550–60. doi: 10.1016/j.ultrasmedbio.2023.02.019.
[91] Paefgen V, Doleschel D, Kiessling F. Evolution of contrast agents for ultrasound imaging and ultrasound-mediated drug delivery. Front Pharmacol 2015;6:197. doi: 10.3389/fphar.2015.00197.
[92] Hwang JA, Jeong WK, Min JH, Kim YY, Heo NH, Lim HK. Sonazoid-enhanced ultrasonography: comparison with CT/MRI Liver Imaging Reporting and Data System in patients with suspected hepatocellular carcinoma. Ultrasonography 2021;40(4):486–98. doi: 10.14366/usg.20120.
[93] Lee SW, Kang MK, Zhang X. Sonazoid contrast-enhanced ultrasonography for the diagnosis of hepatocellular carcinoma: strengths and shortcomings. J Liver Cancer 2023;23(2):238–40. doi: 10.17998/jlc.2023.09.12.
[94] Dave JK, Halldorsdottir VG, Eisenbrey JR, Merton DA, Liu JB, Machado P, et al. On the implementation of an automated acoustic output optimization algorithm for subharmonic aided pressure estimation. Ultrasonics 2013;53(4):880–8. doi: 10.1016/j.ultras.2012.12.010.
[95] Mayer H, Eisenbrey JR, Forsberg F. On microbubble degradation and flow velocity in subharmonic pressure estimation. Ultrasound Med Biol 2025;51(4):722. doi: 10.1016/j.ultrasmedbio.2024.11.001.
[96] Eisenbrey JR, Dave JK, Halldorsdottir VG, Merton DA, Miller C, Gonzalez JM, et al. Chronic liver disease: noninvasive subharmonic aided pressure estimation of hepatic venous pressure gradient. Radiology 2013;268(2):581–8. doi: 10.1148/radiol.13121769.
[97] Gupta I, Eisenbrey JR, Machado P, Stanczak M, Wessner CE, Shaw CM, et al. Diagnosing portal hypertension with noninvasive subharmonic pressure estimates from a US contrast agent. Radiology 2021;298(1):104–11. doi: 10.1148/radiol.2020202677.
[98] Zhu Z, Liang S, Qian L. Noninvasive subharmonic-aided pressure estimation for surgical management of portal hypertension: a clinical study in TIPS patients. Minerva Surg 2025;80(5):381–4. doi: 10.23736/S2724-5691.25.10917-9.
[99] Huang Y, Lu X, Wang F, Cao J, Wang Y, Cheng J, et al. Clinical application of subharmonic aided pressure estimation (SHAPE) in the assessment of portal hypertension in patients with decompensated cirrhosis: a pilot study. Clin Hemorheol Microcirc 2025;89(2):189–97. doi: 10.1177/13860291241304056.
[100] Kuroda H, Abe T, Kamiyama N, Oguri T, Ito A, Nakaya I, et al. Novel subharmonic-aided pressure estimation for identifying high-risk esophagogastric varices. J Gastroenterol 2025;60(2):187–96. doi: 10.1007/s00535-024-02161-4.
[101] Machado P, Gupta I, Fenkel JM, Gummadi S, Stanczak M, Wessner CE, et al. Ultrasound pressure estimation for diagnosing portal hypertension in patients undergoing dialysis for chronic kidney disease. J Ultrasoun Med 2022;41(9):2181–9. doi: 10.1002/jum.15897.
[102] Gupta I, Fenkel JM, Eisenbrey JR, Machado P, Stanczak M, Wessner CE, et al. A noninvasive ultrasound based technique to identify treatment responders in patients with portal hypertension. Acad Radiol. 2021;28(Suppl 1):S128–37 Suppl 1. doi: 10.1016/j.acra.2020.11.023.
[103] Duan Y, Dong B, Li S, Zhang C. Diagnostic accuracy of contrast-enhanced ultrasound for detecting clinically significant portal hypertension and severe portal

hypertension in chronic liver disease: a meta-analysis. Expert Rev Gastroenterol Hepatol 2023;17(5):489–97. doi: 10.1080/17474124.2023.2196402.
[104] Larson AC, Sridharan A, Moon JK, Agarwal D, Chang J, Wallace KD, et al. Contrast-enhanced subharmonic aided pressure estimation for assessment of intracranial pressure in vivo. Pediatr Radiol 2023;53(8):1640–7. doi: 10.1007/s00247-023-05637-2.
[105] Halldorsdottir VG, Dave JK, Eisenbrey JR, Machado P, Zhao H, Liu JB, et al. Subharmonic aided pressure estimation for monitoring interstitial fluid pressure in tumours—in vitro and in vivo proof of concept. Ultrasonics 2014;54(7):1938–44. doi: 10.1016/j.ultras.2014.04.022.
[106] Halldorsdottir VG, Dave JK, Marshall A, Forsberg AI, Fox TB, Eisenbrey JR, et al. Subharmonic-aided pressure estimation for monitoring interstitial fluid pressure in tumors: calibration and treatment with paclitaxel in breast cancer xenografts. Ultrasound Med Biol 2017;43(7):1401–10. doi: 10.1016/j.ultrasmedbio.2017.02.011.
[107] Wang Y, Lu H, Huang L, Li D, Qiu W, Li L, et al. Noninvasive estimation of tumor interstitial fluid pressure from subharmonic scattering of ultrasound contrast microbubbles. Biosensors (Basel) 2023;13(5). doi: 10.3390/bios13050528.
[108] Nam K, Eisenbrey JR, Stanczak M, Sridharan A, Berger AC, Avery T, et al. Monitoring neoadjuvant chemotherapy for breast cancer by using three-dimensional subharmonic aided pressure estimation and imaging with US contrast agents: preliminary experience. Radiology 2017;285(1):53–62. doi: 10.1148/radiol.2017161683.
[109] Wessner CE, Pomeranz C, Blackman R, Hoy MK, Bradigan K, Stache SA, et al. Noninvasive diagnosis of chronic exertional compartment syndrome with shear wave elastography and subharmonic aided pressure estimation. J Ultrasound Med 2025. doi: 10.1002/jum.70030.
[110] Nam K, Torkzaban M, Shames JP, Liao L, Wessner CE, Machado P, et al. Characterization of indeterminate breast lesions based on pressure estimates by noninvasive 3d contrast-enhanced ultrasound. Ultrasound Med Biol 2024;50(12):1854–60. doi: 10.1016/j.ultrasmedbio.2024.08.010.
[111] Forsberg F, Piccoli CW, Sridharan A, Wilkes A, Sevrukov A, Ojeda-Fournier H, et al. 3D harmonic and subharmonic imaging for characterizing breast lesions: a multicenter clinical trial. J Ultrasound Med 2022;41(7):1667–75. doi: 10.1002/jum.15848.
[112] Sridharan A, Eisenbrey JR, Stanczak M, Machado P, Merton DA, Wilkes A, et al. Characterizing breast lesions using quantitative parametric 3D subharmonic imaging: a multicenter study. Acad Radiol 2020;27(8):1065–74. doi: 10.1016/j.acra.2019.10.029.
[113] Forsberg F, Stanczak M, Lyshchik A, Loren D, O'Kane P, Siddiqui A, et al. Subharmonic and endoscopic contrast imaging of pancreatic masses: a pilot study. J Ultrasound Med 2018;37(1):123–9. doi: 10.1002/jum.14310.
[114] Gupta I, Freid B, Masarapu V, Machado P, Trabulsi E, Wallace K, et al. Transrectal subharmonic ultrasound imaging for prostate cancer detection. Urology 2020;138:106–12. doi: 10.1016/j.urology.2019.12.025.
[115] Delaney LJ, Machado P, Torkzaban M, Lyshchik A, Wessner CE, Kim C, et al. Characterization of adnexal masses using contrast-enhanced subharmonic imaging: a pilot study. J Ultrasound Med 2020;39(5):977–85. doi: 10.1002/jum.15183.
[116] Goertz DE, Frijlink ME, Tempel D, Bhagwandas V, Gisolf A, Krams R, et al. Subharmonic contrast intravascular ultrasound for vasa vasorum imaging. Ultrasound Med Biol 2007;33(12):1859–72. doi: 10.1016/j.ultrasmedbio.2007.05.023.
[117] Li R, Zhang Y, Zheng S, Zhang W, Du K, He W. Biomechanical characteristics in the carotid artery: noninvasive assessment using subharmonic emissions from microbubbles. Med Phys 2023;50(11):6857–63. doi: 10.1002/mp.16542.
[118] Li R, Zhang Y, Zheng S, Cheng L, Chen Z, He W, et al. Noninvasive assessment of carotid plaque with subharmonic aided pressure estimation from a US contrast agent: a preliminary study. Clin Transl Sci 2023;16(3):502–11. doi: 10.1111/cts.13465.
[119] Wang P, Tan C, Ji X, Bai J, Yu ACH, Qin P. Sensitivity improvement of subharmonic-based pressure measurement using phospholipid-coated monodisperse microbubbles. Ultrason Sonochem 2024;104:106830. doi: 10.1016/j.ultsonch.2024.106830.